JCTC Journal of Chemical Theory and Computation

Structural Optimization of Silver Clusters up to 80 Atoms with Gupta and Sutton-Chen Potentials

Xueguang Shao,* Xiaomeng Liu, and Wensheng Cai

Department of Chemistry, University of Science and Technology of China, Hefei, Anhui 230026, P.R. China

Received December 6, 2004

Abstract: The structure of silver clusters containing up to 80 atoms is optimized by using a random tunneling algorithm (RTA). The Gupta-type many-body potential and the Sutton-Chen (SC) many-body potential are used to account for the interactions among the atoms in the cluster, respectively. It is found that many of the structural configurations optimized with the two potentials are different, especially at a small size, and the structures with the Gupta potential are highly strained and apt to be the disordered motifs, whereas the structures with the SC potential are less-strained and the ordered morphologies are more favorable. Due to the difference of long-range interaction and pair contribution between two potentials, the assignment of outermost-shell atoms in decahedron and the missing atoms on the surface of the icosahedral motifs are also different for the two potentials. Furthermore, a new global minimum of the 68-atom silver cluster with the decahedral motif is found for both two potential models.

1. Introduction

Clusters provide a bridge between a few atoms or molecules and the bulk materials and show unique aspects of chemical and physical properties.[1] Therefore, studies on microclusters have increased rapidly in both experimental[2] and theoretical[3−5] investigations. In recent years, metal clusters gradually become a hotspot in cluster studies,[6] and silver clusters are particularly interesting.[7−17] First, silver clusters and small particles have practical importance in photography[7] and catalysis,[8] including their potential use in new electronic materials.[9] Second, adsorbates on silver surfaces seem to have a cluster counterpart observed by the enhanced Raman effect.[10] Also, silver clusters play an important role in metal alloy clusters.[11,16]

The geometry structure is a key property of a cluster in understanding the transition from the microscopic structure to the macroscopic structure of material. The most stable structure often possesses the lowest potential energy. Until now, large numbers of theoretical simulations have been done on the subject of silver clusters. For metal clusters, because of the *d* electrons and shell effect,[6] interaction between two atoms depends on not only distance but also local surroundings. Therefore, simple pairwise potential, such as Lennard-Jones (LJ) potential, is not suitable for metal clusters. It is widely recognized that empirical many-body potentials provide with good accuracy on the structural and thermodynamic properties of most transition metals. Wales et al.[18] also proved that many-body potential models play a crucial role in metal clusters.

Lots of empirical many-body potentials have been introduced for the global optimization of metal clusters, such as the Gupta potential,[19] the Sutton-Chen (SC) potential,[20,21] the Erkoc potential,[22] and so on. They had been widely used in the optimization of Ag, Au, Zn, Cd, Ni, and Cu[13−17,23−27] clusters. However, up to now, no single potential function model can totally reflect the structural motifs of silver clusters obtained by experiment. Therefore, the comparison of different potentials is necessary and important.

In this work, two commonly used potentials, the Gupta potential model and the SC potential model, were adopted in the global optimization of silver clusters to seek for further understanding of the potentials and the parameters in metal cluster simulation. The putative global minima of silver clusters up to 80 atoms are found by using an effective random tunneling algorithm (RTA)[28] with the two potential

* Corresponding author phone: +86-551-3606160; fax: +86-551-3601592; e-mail: xshao@ustc.edu.cn.

10.1021/ct049865j CCC: $30.25
Published on Web 06/07/2005

models. By comparison of the results, it is found that the assignments of outer-shell atoms are different in the decahedral and icosahedral structures for the two potentials. Furthermore, the growth patterns at smaller size are also found to be different. Moreover, a new global minimum with decahedral motif of 68-atom silver clusters is found for both two potentials.

2. Method

2.1. Potential Models. The Gupta potential[19] is based on the second moment approximation of the electron density of states in the tight-binding (TB) theory and is depicted in the following form

$$V = \frac{U_n}{2}\sum_{i=1}^{n} V_i \tag{1}$$

where n is the number of atoms in the cluster, and

$$V_i = \left[A\sum_{j\neq i}\exp\left[-p\left(\frac{r_{ij}}{r_0}-1\right)\right] - \left(\sum_{j\neq i}\exp\left[-2q\left(\frac{r_{ij}}{r_0}-1\right)\right]\right)^{1/2}\right] \tag{2}$$

r_{ij} is the distance between atoms i and j and r_0 is the equilibrium nearest-neighbor distance in the bulk metal. The parameters p and q represent the repulsive interaction range and the attractive interaction range, respectively. The parameter A is fitted to experimental values of the cohesive energy. U_n is a function of the atom number n. In eq 2, the first term gives a pairwise repulsion energy of the Born−Mayer type, and the second term represents the n-body attractive contribution.

The Sutton-Chen (SC) potential[20] is described by eq 3

$$E = \epsilon\sum_i\left[\frac{1}{2}\sum_{j\neq i}\left(\frac{\alpha}{r_{ij}}\right)^n - c\sqrt{\rho_i}\right] \tag{3}$$

where

$$\rho_i = \sum_{j\neq i}\left(\frac{\alpha}{r_{ij}}\right)^m \tag{4}$$

r_{ij} is the distance between atoms i and j. The constant α is the bulk lattice constant, c is a dimensionless parameter, ϵ is a parameter with dimensions of energy, and the exponents n and m are integers. They are also the key parameters determining the repulsive and the attractive interaction range. All of the above parameters are obtained by fitting to the 0 K properties of metals. Similarly, the potential energy is also given as a sum of a pairwise repulsion term and a many-body density dependent cohesion term.

The values of the parameters in the above equations used in the work are listed in Table 1.[14,25] In the following calculations, the reduced units with $r_0 = 1$, $U_n = 1$, $\epsilon = 1$, and $\alpha = 1$ are adopted.

2.2. Global Optimization Method. A global optimization algorithm called random tunneling algorithm (RTA)[28] is used to deal with the problem of searching the lowest minima of silver clusters. The RTA is derived from the terminal repeller unconstrained subenergy tunneling (TRUST) algorithm. TRUST is a deterministic global optimization approach that has been successfully used in exploratory seismology.[29,30] Based on the subenergy tunneling technique of TRUST, the stochastic algorithm RTA was developed for the purpose of solving multi- or high-dimensional global optimization problems. RTA has two optimization phases, a global phase and a local phase. The global phase is also termed the tunneling phase, in which the global sampled points are generated by a random tunneling technique. In the local phase, the gradient method limited memory BFGS (LBFGS)[31] is applied to these points, yielding various local optima. The procedure of RTA can be summarized in two steps, i.e., first, a population of configurations is generated covering the whole solution space and then the random tunneling and local minimization are executed circularly until the global minimum is found or the circulatory count reaches a preset value. The efficiency of RTA has been investigated with a set of standard multidimensional test functions.[28] By comparison of the RTA with some well-known global optimization methods, it was shown that the algorithm is efficient for searching the multidimensional problem. The algorithm was also applied to the structural optimization of LJ clusters and successfully located the lowest known minima containing up to 100 atoms.[28] Furthermore, all the known minima of LJ clusters with the size lower than 330 were successfully located by the parallelization of the RTA with the improved seeding technique.[32] A more detailed description of the algorithm can be found in refs 28 and 32.

Table 1. Parameters Used in the Gupta and Sutton-Chen Potential Models for Silver Clusters

Gupta potential			Sutton-Chen potential		
A	*p*	*q*	*c*	*n*	*m*
0.09944	10.12	3.37	144.41	12	6

3. Results and Discussion

3.1. The Optimization Results of Silver Clusters up to 80 Atoms. The optimized results, including the potential energies and the structural configurations of the global minima of the silver clusters up to 80 atoms, are summarized in Table 2. It can be seen that the structural motifs obtained with the two potential models are different at many cluster sizes. This implies that the potential model plays an important role in the structural configuration.

The structural motifs of silver clusters for each size containing up to 80 atoms optimized with the Gupta potential are shown in Figure 1. In the magic number sequence, such as the size $n = 13$, 19, 38, 55, and 75, the same structures are found by using the two potentials and also the same from $n = 6$ to 13. Except for the eight-atom dodecahedron, the structures between 6 and 13 lead to a growth sequence to a complete 13-atom icosahedron. From the size $n = 15$ to 47, most of the optimized structural motifs with the two potentials are different. It shows the different growth patterns of the silver clusters with the two potentials. This will be discussed in detail in the next section. From the size $n = 55$ to 75, silver clusters complete the transform from icosahedron

Table 2. Global Minima for Silver Clusters Optimized by the Gupta Potential and the Sutton-Chen Potential[a]

Gupta potential						Sutton-Chen potential					
N	energy	SD	N	energy	SD	N	energy	SD	N	energy	SD
3	−2.175900		42	−43.029888	dis	3	−1704.6905		42	−39301.6696	M
4	−3.211187		43	−44.110792	d4	4	−2601.8447		43	−40341.8543	M
5	−4.197445		44	−45.199405	dis	5	−3461.3452		44	−41310.9157	M
6	−5.236519		45	−46.249608	dis	6	−4378.8875		45	−42345.0912	d4
7	−6.238864		46	−47.359604	dis	7	−5271.2947		46	−43436.2827	M
8	−7.212287		47	−48.410801	dis	8	−6129.7564		47	−44405.1884	M
9	−8.230424		48	−49.549968	d4	9	−7048.7552		48	−45470.1069	d4
10	−9.249730		49	−50.614913	M	10	−7972.0971		49	−46521.2131	M
11	−10.258679		50	−51.701995	c	11	−8889.9627		50	−47518.6719	c
12	−11.305364		51	−52.725760	M	12	−9871.2458		51	−48522.4267	M
13	−12.472315	M	52	−53.867489	M	13	−10968.5082	M	52	−49616.1377	M
14	−13.406669	aM	53	−54.995380	M	14	−11798.8479	aM	53	−50706.4665	M
15	−14.455938	da	54	−56.142189	M	15	−12742.9841	aM	54	−51796.0777	M
16	−15.481217	dis	55	−57.255433	M	16	−13672.6475	aM	55	−52884.6808	M
17	−16.520324	dis	56	−58.205738	aM	17	−14606.3231	aM	56	−53756.6516	aM
18	−17.544132	dis	57	−59.256129	d5	18	−15535.3810	aM	57	−54700.1733	aM
19	−18.621146	aM	58	−60.361585	aM	19	−16595.0561	aM	58	−55753.8515	aM
20	−19.627271	aM	59	−61.395937	d5	20	−17510.9209	aM	59	−56751.4572	c
21	−20.678291	dis	60	−62.499086	aM	21	−18433.0300	aM	60	−57763.6760	aM
22	−21.757355	dis	61	−63.614111	aM	22	−19422.7209	dis	61	−58809.0448	aM
23	−22.809005	dis	62	−64.675376	d5	23	−20383.3977	dis	62	−59765.2180	aM
24	−23.835809	dis	63	−65.787033	d5	24	−21315.4208	h	63	−60822.3826	d5
25	−24.865922	dis	64	−66.946249	d5	25	−22339.6319	d3	64	−61925.6244	d5
26	−25.942226	dis	65	−67.985547	d5*	26	−23337.2211	h	65	−62903.7387	d5
27	−27.014674	dis	66	−69.074581	d5	27	−24284.3891	h	66	−63959.3105	d5
28	−28.082239	dis	67	−70.201134	d5	28	−25276.9501	M	67	−65011.2767	d5
29	−29.128461	dis	68	−71.273853	d5	29	−26263.2779	d4	68	−65983.2888	d5
30	−30.204287	dis	69	−72.334831	d5*	30	−27253.8536	d3	69	−67020.4042	d5
31	−31.260336	dis	70	−73.465005	d5	31	−28274.4371	d4	70	−68114.9462	d5
32	−32.331501	dis	71	−74.620916	d5	32	−29265.3320	M	71	−69216.6518	d5
33	−33.387556	d4*	72	−75.659788	d5*	33	−30274.9603	d4	72	−70171.4663	d5
34	−34.444690	dis	73	−76.752234	d5	34	−31231.7697	c	73	−71225.8547	d5
35	−35.536870	dis	74	−77.880111	d5	35	−32280.3945	d4	74	−72318.7243	d5
36	−36.587712	dis	75	−79.037373	d5	36	−33253.9352	M	75	−73421.0521	d5
37	−37.685406	d4	76	−80.075806	d5*	37	−34302.6067	c	76	−74375.6975	d5
38	−38.820496	f	77	−81.170022	d5	38	−35419.9804	f	77	−75430.9852	d5
39	−39.858635	f	78	−82.209914	d5*	39	−36364.8587	f	78	−76385.4318	d5
40	−40.896664	f	79	−83.337830	c	40	−37324.3708	M	79	−77456.0255	c
41	−41.960532	d4	80	−84.365961	d5	41	−38316.5698	c	80	−78414.6271	c

[a] The structural distribution (SD) are as follows: decahedral with *n* atoms along the decahedral axis (dn); icosahedral with a Mackay (M) or an anti-Mackay (aM) overlayer; disordered morphologies (dis); closed-packed fcc (f), hcp (h), a mixture of stacking sequences and twin planes (c); clusters with disclination axis (da). Different atom assignments are marked with * in the Gupta decahedral.

to decahedron, leading from the complete 55-atom Mackay icosahedron to the 75-atom Marks decahedron. This provides a validation of the structural transformation reported before.[17,18,25]

The comparison of the finite difference of the energy ΔE and the second finite difference of the energy $\Delta_2 E$ with the two potentials are plotted in Figure 3(a),(b). The ΔE and $\Delta_2 E$ have the form as follows

$$\Delta E(n) = E(n) - E_J(n) \tag{5}$$

where

$$E_J(n) = a + bn^{1/3} + cn^{2/3} + dn$$

$$\Delta_2 \mathrm{E}(n) = E(n+1) + E(n\text{-}1) - 2E(n) \tag{6}$$

$E_J(n)$ is a four-parameter fit of the energy of global minimum. $\Delta_2 E$ measures the stability of an *n*-atom cluster structure with respect to its neighboring cluster size. It can be seen that the Gupta and the SC results have similar shape. Valleys in ΔE and peaks in $\Delta_2 E$ are both in well accord with the magic numbers observed in mass spectra.[33] This also explains the stability of the magic number clusters. In a few different inflection points in the figure, different structural motifs or different atom assignment are found for the two potentials correspondingly.

At the 68-atom cluster size, a close-packed structure motif (Figure 2a) had been reported.[25] In this work, a new global minimum is found with a decahedral motif (Figure 2b) for both potentials. The energy of $(Ag)_{68}$ in this work with the SC potential is -65983.2888ϵ, which is lower than the energy -65980.5983ϵ in ref 25. Furthermore, the global minimum at 68-atom cluster size is also found to be the decahedral motif for the Gupta potential. Although the new

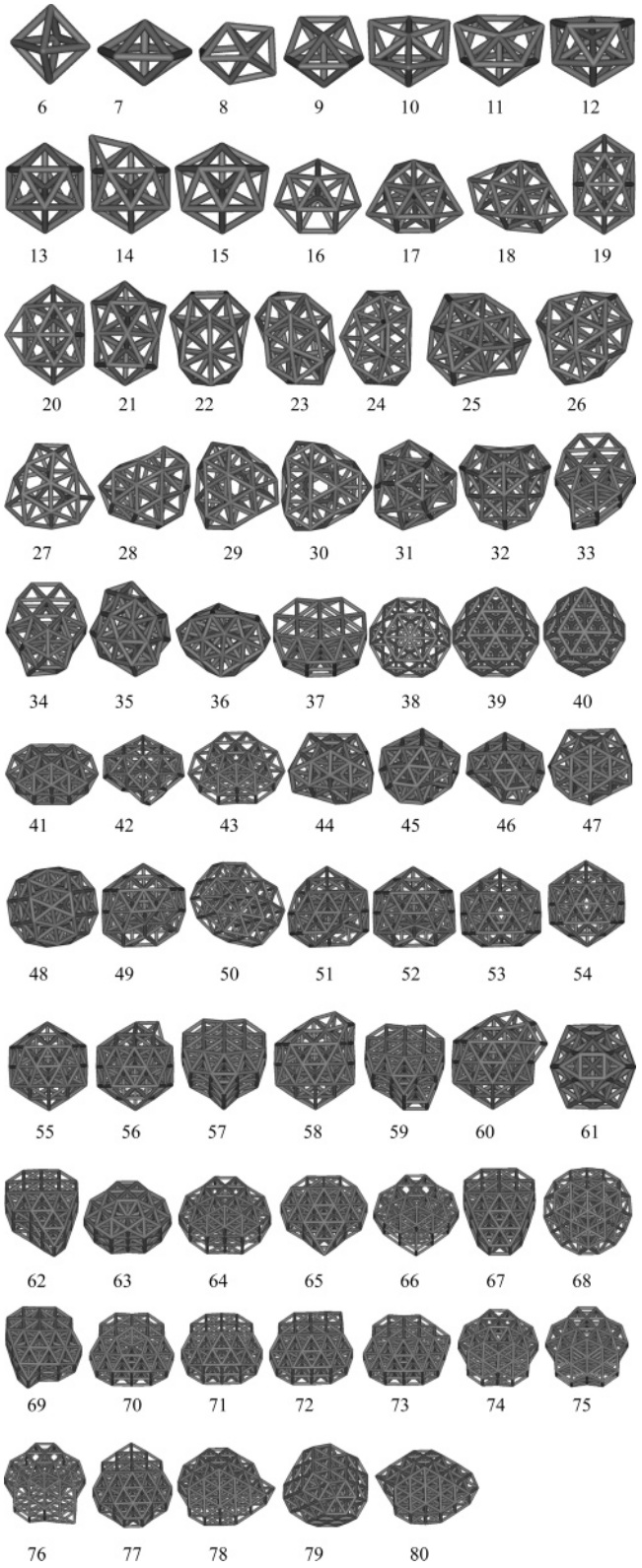

Figure 1. Structures of the global energy minima for silver clusters with the Gupta potential.

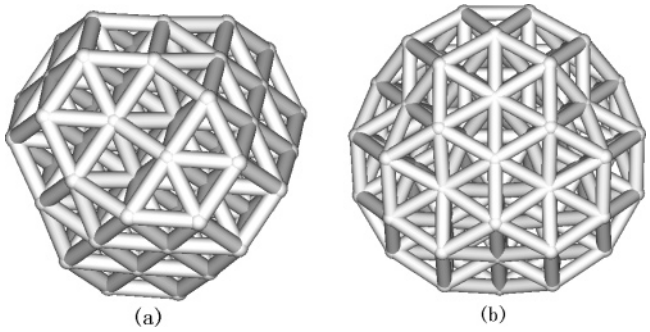

Figure 2. The global energy minima of a 68-atom silver cluster. (a) Closed-packed structure from ref 25. (b) Decahedral structure with the Sutton-Chen and the Gupta potential.

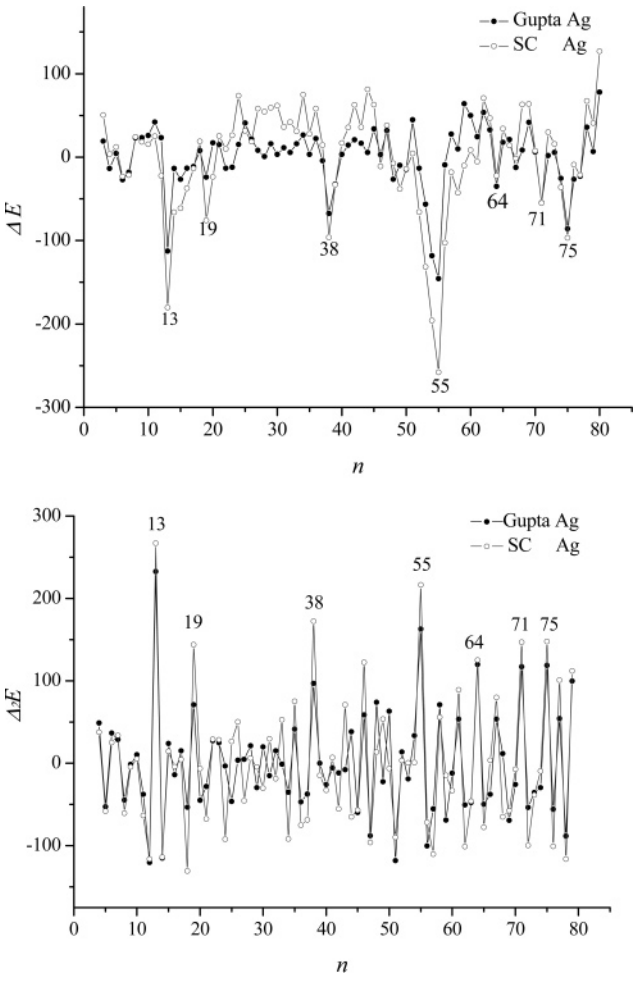

Figure 3. Stability analysis of Ag clusters: (a) the comparison of ΔE for two potentials and (b) the comparison of $\Delta_2 E$ for two potentials. $E_J(n) = 1.5859 - 1.54692n^{1/3} + 1.03058n^{2/3} - 1.23123n$ for the Gupta potential, where the coefficients are obtained by the best fit to the energies of the global minima; $E_J(n) = 940.63759 - 994.91694n^{1/3} + 1126.623n^{2/3} - 1201.40809n$ for the Sutton-Chen potential, the same way to get the coefficients.

global minimum is not so stable in comparison with the magic number clusters, it can be seen from Figure 3 that the new SC-68 cluster is actually in a relative stable position, especially compared with its isomer found before.

3.2. Growth Patterns at Smaller Size of Silver Clusters. From Table 2, it can be seen that a big difference between the results of the two potentials exist in the range $n = 15$ to 47. In this range, the silver cluster structures with the two potentials are different except the size $n = 19$, 20, 22, 38, and 39. Most of the Gupta results are disordered morphologies, but the SC results are mostly ordered structures. The

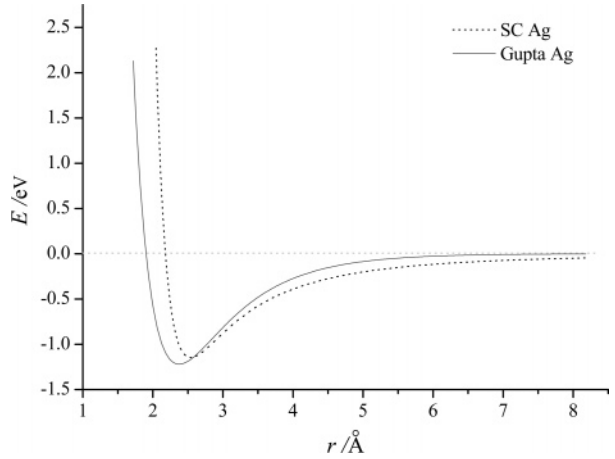

Figure 4. Plots of the Gupta potential and the Sutton-Chen potential for the diatomic interaction of silver clusters.

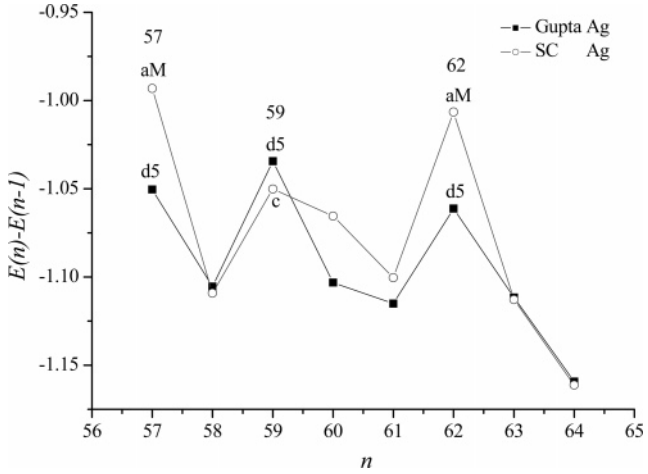

Figure 5. $E(n) - E(n-1)$ versus the number of the atom n from 57 to 64 for the Gupta potential and the Sutton-Chen potential.

15-atom cluster displays a unique motif with a disclination axis and the central atom connects with the other 14 atoms. As shown in Figure 1, from $n = 16$ to 18, the global minima of the Gupta potential are based on distorted decahedra, however, that of the SC potential grow with an anti-Mackay icosahedral pattern. The structures with the Gupta potential from $n = 21$ to 30 are based on the distorted face-sharing icosahedra and disordered in various ways. From the size $n = 42$ to 47, the Gupta clusters grow with a distorted incomplete Mackay icosahedral pattern except for the d4 decahedral motif of the 43-atom cluster.

The motifs of 19-, 20-, 22-, 38-, and 39-atom clusters in the range 15−47 (as shown in Figure 1) are the only five same structures optimized by the two potentials, corresponding to a 19-atom double icosahedron, a 38-atom truncated octahedron, and their derivants, respectively. The Gupta 41-atom global minimum is a decahedron with 4 atoms along the decahedral axis; however, the structure with the SC potential of the 41-atom silver cluster displays the close-packed configuration. Interestingly, this close-packed structure is also obtained by the Gupta potential with a little higher energy than the Gupta 41-atom global minimum.

Clearly, the structural configurations show the different growth patterns with the two potential models at smaller size. To explain the differences, the interactions of a dimer expressed by the two potentials are plotted in Figure 4. It can be seen that the bottom of the Gupta potential is broad, whereas it is narrow and sharp for the SC potential. The Gupta potential model can be more tolerant of strain than the SC potential model. The structures with the Gupta potential are highly strained, near spherical, and not based on regular packing, while those with the SC potential are less-strained, and the ordered morphologies are more favorable. Therefore, these differences bring to the different growth patterns. At smaller size, most of the structures obtained by the Gupta potential model display the disordered motifs because this configuration is highly strained, whereas the ordered motifs are more preferable for the SC potential model because it is less strained. Lots of theoretical[14,34,35] and experimental[36] works have been investigated to explain the growth patterns at smaller size. The studies suggest that the global minima show disordered structures at a smaller size, but they will disappear at a larger size. Most of the disordered structures are more spherical and have a larger number of nearest-neighbor contacts, and this makes them become more stable than the ordered morphologies. But it does not exist at larger size because of the energetic penalty for the strain scales with the volumes.[25,34]

3.3. Structural Motifs in the Transition from Icosahedron to Decahedron. As shown in Figure 1, there is transition from icosahedra to decahedra between the size $n = 55$ to 75. The SC results lead to a decahedral growth sequence from the 63-atom cluster and for the Gupta results from the size 62. Interestingly, the SC results complete the transform from 62 to 63; however, the Gupta structures alternate between the two conformations from 57 to 61. The structural stability in the transition is plotted as $E(n) - E(n-1)$ versus the number of the atoms n in Figure 5. Peaks in two curves correspond to the different structures optimized by the two potentials, which are both unstable. In the transition, two conformations have fierce competition, and their energy differences are extremely small. Therefore, different structural motifs of the global minimum are found. It can be found that the crossover between icosahedron and decahedron is a gradual process. Silver clusters in the transition may have the concurrent motifs until one motif becomes the preferential conformation.

3.4. Assignment of the Outermost-Shell Atoms in Decahedron or Icosahedron. At several sizes, the global minima of silver clusters with both two potentials are similar, such as the 33-, 65-, 69-, 72-, 76-, and 78-atom decahedra and the 51-, 52-, 53-, and 54-atom icosahedra. However their assignments of the outermost-shell atoms are different. The projection-drawings of 65-, 72-, 76-, 78-atom decahedral structures with the two potentials are shown in Figure 6. From the figure it can be found that the motifs optimized by the Gupta potential have a common property, i.e., the atom marked with a black ball is apt to be located in the furthest shell of the decahedral morphologies. Contrarily, the SC results display a distribution of another pattern, where the atom first fills in the vacancy of a relative inner shell of the decahedral motif. From Figure 4, it can be found that

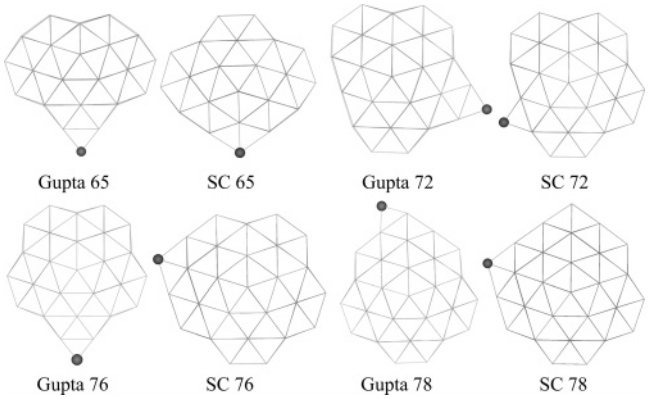

Figure 6. The projection drawings of different atom assignments on the decahedral surface of the 65-, 72-, 76-, and 78-atom Ag clusters.

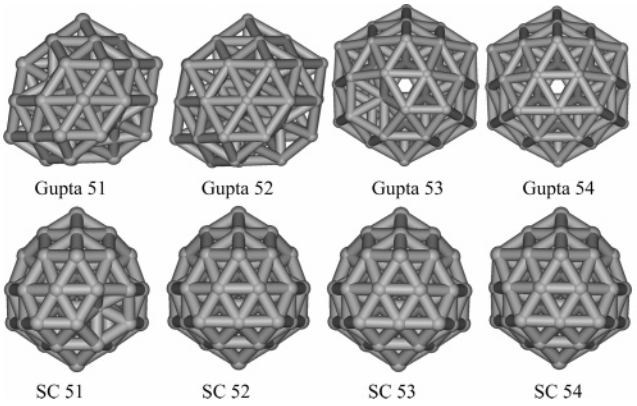

Figure 7. The structural motifs with different missing atoms on the icosahedral surface of 51-, 52-, 53-, and 54-atom Ag clusters.

the long-range interaction (far from the equilibrium position) of the SC potential model is stronger than that of the Gupta potential model. The energy of the Gupta potential model quickly approaches to zero and its long-range interaction is weak. Therefore, the strain energy play a more important role in the configuration of the Gupta potential than that of the SC potential.[34] The single atom (marked with a black ball in Figure 6) will easily grow to the furthest shell for the Gupta potential because in this configuration the four nearest atoms are in a plane so that there is almost no tensile force. On the contrary, under the SC potential, the single atom will be located not in the furthest shell but in the relative inner shell because the strain energy has not so much effect on its configuration. This should be the reason that causes the difference of the outermost-shell atom assignment in Figure 6.

Similarly, in the growth toward the 55-atom complete Mackay icosahedron, the structures obtained by the two potentials also display different patterns. The 51-, 52-, 53-, and 54-atom icosahedral structures described by the two potential models are shown in Figure 7. It can be seen that the missing atoms on the surface of the icosahedral motifs of the SC results are symmetrically distributed but that of the Gupta results are not. Interestingly, the structures of the Gupta results show the central atom vacancy (there is no atom at the center of icosahedron) at the sizes 53 and 54. In LJ clusters, there shows the central vacancy in icosahedron in the range $561 \leq n \leq 923$.[37] Also, the central vacancy has existed in different metal clusters.[15] The study finds that at large sizes, the icosahedron of silver cluster with central vacancy will become the dominant morphology. The global minimum of the 54-atom aluminum cluster also shows a hollow icosahedron.[38] The contraction of the inner shells for the icosahedral structure leads to a strong pressure on the central core. When the central atom energy is higher than that of the atom on edges and faces of the outermost shell, the central atom will escape from the central site to the surface sites of the outer layer. This reason causes the competition between hollow and centered icosahedral structures. Due to the difference of the pair contribution to the two potential models, which leads to the different compression to the center, there displays hollow and centered icosahedral motifs of 53- and 54-atom clusters for the Gupta potential and the SC potential, respectively.

4. Conclusion

Two empirical potentials frequently applied in the description of metal clusters are used to find the structural motifs of silver clusters with the atom numbers up to 80. By comparison of the results optimized with the Gupta and the SC potential, respectively, it was found that the potential model has a great influence on the global minima of silver clusters. The structures of the global minima for the two potentials have different growth patterns in the range 15−47. The structures with the Gupta potential are highly strained and apt to be the disordered motifs, whereas the structures with the SC potential are less-strained and the ordered morphologies are more favorable. Through the comparison of the structures in the transition from icosahedron to decahedron with the two potentials, it can be found that the crossover between icosahedron and decahedron is a gradual process. Different structures in this transition have fierce competition that there may have the concurrent motifs. Due to the reason that two potentials have different long-range interactions and have a different pair contribution, atom assignments on the surface of decahedra and icosahedra are different. At the 68-atom silver cluster, a new lowest energy minimum of decahedral motif is found by using the two potentials.

Acknowledgment. This study is supported by the outstanding youth fund (No. 20325517) from National Natural Scientific Foundation of China (NNSFC) and the Teaching and Research Award Program for Outstanding Young Teachers (TRAPOYT) in higher education institutions of the Ministry of Education (MOE), P. R. China.

References

(1) Wales, D. J.; Scheraga, H. A. *Science* **1999**, *285*, 1368−1372.

(2) Chesnovsky, O.; Taylor, K. J.; Conceicao, J.; Smalley, R. E. *Phys. Rev. Lett.* **1990**, *64*, 1785−1788.

(3) Shao, X. G.; Cheng, L. J.; Cai, W. S. *J. Comput. Chem.* **2004**, *25*, 1693−1698.

(4) Xiang, Y. H.; Jiang, H. Y.; Cai, W. S.; Shao, X. G. *J. Phys. Chem. A* **2004**, *108*, 3586−3592.

(5) Hartke, B. *Struct. Bond.* **2004**, *110*, 33−53.

(6) Alonso, J. A. *Chem. Rev.* **2000**, *100*, 637−677.

(7) Eachus, R. S.; Marchetti, A. P.; Muenter, A. A. *Annu. Rev. Phys. Chem.* **1999**, *50*, 117−144.

(8) Koretsky, G. M.; Knickelbein, M. B. *J. Chem. Phys.* **1997**, *107*, 10555−10566.

(9) Kim, S. H.; Medeiros-Ribeiro, G.; Ohlberg, D. A. A.; Stanley Williams, R.; Heath, J. R. *J. Phys. Chem. B* **1999**, *103*, 10341−10347.

(10) Chan, W. T.; Fournier, R. *Chem. Phys. Lett.* **1999**, *315*, 257−265.

(11) Lee, I.; Han, S. W.; Kim, K. *Chem. Commun.* **2001**, *18*, 1782−1783.

(12) Fournier, R. *J. Chem. Phys.* **2001**, *115*, 2165−2177.

(13) Erkoc, S.; Yilmaz, T. *Physica E* **1999**, *5*, 1−6.

(14) Michaelian, K.; Rendon, N.; Garzon, I. L. *Phys. Rev. B* **1999**, *60*, 2000−2010.

(15) Mottet, C.; Treglia, G.; Legrand, B. *Surf. Sci. Lett.* **1997**, *383*, L719−L727.

(16) Johnston, R. L. *Dalton Trans.* **2003**, 4193−4207.

(17) Baletto, F.; Mottet, C.; Ferrando, R. *Phys. Rev. B* **2001**, *63*, 155408(10).

(18) Uppenbrink, J.; Wales, D. J. *J. Chem. Phys.* **1992**, *96*, 8520−8534.

(19) Gupta, R. P. *Phys. Rev. B* **1981**, *23*, 6265−6270.

(20) Sutton, A. P.; Chen, J. *Philos. Mag. Lett.* **1990**, *61*, 139−146.

(21) Rafiitabar, H.; Sutton, A. P. *Philos. Mag. Lett.* **1991**, *63*, 217−224.

(22) Erkoc, S. *Phys. Status Solidi B* **1992**, *171*, 317−324.

(23) Darby, S.; Mortimer-Jones, T. V.; Johnston, R. L.; Roberts, C. *J. Chem. Phys.* **2002**, *116*, 1536−1550.

(24) Baletto, F.; Ferrando, R.; Fortunelli, A.; Montalenti, F.; Mottet, C. *J. Chem. Phys.* **2002**, *116*, 3856−3863.

(25) Doye, J. P. K.; Wales, D. J. *New J. Chem.* **1998**, *22*, 733−744.

(26) Cagin, T.; Dereli, G.; Uludogan, M.; Tomak, M. *Phys. Rev. B* **1999**, *59*, 3468−3473.

(27) Cleri, F.; Rosato, V. *Phys. Rev. B* **1993**, *48*, 22−33.

(28) Jiang, H. Y.; Cai, W. S.; Shao, X. G. *Phys. Chem. Chem. Phys.* **2002**, *4*, 4782−4788.

(29) Barhen, J.; Protopopescu, V.; Reister, D. *Science* **1997**, *276*, 1094−1097.

(30) Cetin, B. C.; Barhen, J.; Burdick, J. W. *J. Optimiz. Theory App.* **1993**, *77*, 97−126.

(31) Liu, D. C.; Nocedal, *J. Math. Progm.* **1989**, *45*, 503−528.

(32) Shao, X. G.; Jiang, H. Y.; Cai, W. S. *J. Chem. Inf. Comput. Sci.* **2004**, *44*, 193−199.

(33) Clemenger, K. *Phys. Rev. B* **1985**, *32*, 1359−1362.

(34) Doye, J. P. K.; Wales, D. J.; Berry, R. S. *J. Chem. Phys.* **1995**, *103*, 4234−4249.

(35) Wetzel, T. L.; DePristo, A. E. *J. Chem. Phys.* **1996**, *105*, 572−580.

(36) Alameddin, G.; Hunter, J.; Cameron, D.; Kappes, M. *Chem. Phys. Lett.* **1992**, *192*, 122−128.

(37) Shao, X. G.; Xiang, Y. H.; Cai, W. S. *Chem. Phys*. **2004**, *305*, 69−75.

(38) Lioyd, L. D.; Johnston, R. L.; Roberts, C.; Mortimer-Jones, T. V. *Chem. Phys. Chem.* **2002**, *3*, 408−415.

CT049865J